

# Enhanced backscattering from a volume-scattering medium behind a phase screen

Aristide Dogariu and Glenn D. Boreman

Center for Research and Education in Optics and Lasers, University of Central Florida, Orlando, Florida 32816

Madi Dogariu

Department of Physics, University of Central Florida, Orlando, Florida 32816

Received April 10, 1995

The enhanced-backscattering (EBS) phenomenon is investigated for the case in which a phase screen is placed close to a multiple-scattering medium. This situation results in a narrowing of the EBS peak that depends on the strength and the position of the phase screen. The resulting enhancement peak is essentially the sum of two contributions: the EBS produced by the multiple-scattering medium in the absence of the phase screen and the enhancement obtained when the multiple-scattering medium is replaced by a plane mirror. © 1995 Optical Society of America

The effect of electromagnetic-wave propagation through a random phase screen is thoroughly discussed in the context of optical imaging.<sup>1</sup> However, phase-screen models are used to describe the backscattering enhancement that results from the double passage of light through large-scale turbulences.<sup>2,3</sup> In this Letter we approach the problem of enhanced backscattering (EBS) produced by a volume-scattering medium (VSM) that is placed behind a random-phase screen (RPS). This situation could be encountered in many practical applications in atmospheric scattering or in scattering from biological media.

The phenomenon of EBS from a VSM is well understood theoretically, and the effects of various experimental parameters have been investigated.<sup>4-6</sup> When a collimated laser beam impinges upon a VSM as in Fig. 1a, the photons are retroreflected after they have traveled along a large number of independent scattering paths. The spatial distribution of the scattered intensity has the appearance of random interference (speckle). This interference averages out if the relative positions of the scattering centers change over distances of the order of a wavelength, except for the interference of those emerging waves that propagate close to the backward direction and that have traveled along the same light path but in opposite directions. As can be seen from Fig. 1a, photons that have traveled along time-reversed paths will always be in phase. The corresponding far-field intensity is of the form of  $\cos[(\mathbf{k}_f + \mathbf{k}_i) \cdot (\mathbf{r}_f - \mathbf{r}_i)]$ , where  $\mathbf{k}_i$  and  $\mathbf{k}_f$  denote the incident and emergent wave vectors, respectively. This interference is controlled by the average interparticle distance  $l^* \propto \langle |\mathbf{r}_i - \mathbf{r}_f| \rangle$ . Consequently a cone of enhanced intensity with an angular width of  $\sim \lambda/l^*$  develops around the backward direction. The enhancement cone can be regarded as the result of an azimuthal averaging of the interference patterns corresponding to pairs of coherent sources separated by a distance  $l^*$ .

A similar effect of EBS around the direction of incidence can be observed when a RPS is placed a distance  $d$  from a mirror as in Fig. 1b. This time

the corresponding separation distance between the end points of the time-reversed scattering sequences,  $\langle |\mathbf{r}_i - \mathbf{r}_f| \rangle$ , is determined by the transverse scattering length  $\delta = 2dm$ , where  $m$  is the angular deviation introduced by the RPS. If we consider a thin RPS determined by a distorted interface of mean slope  $\epsilon$  that separates media with the refractive indices  $n_1$  and  $n_2$ , the average angular deviation produced by the RPS is  $\epsilon(n_1/n_2 - 1)$ . For small separations  $d$ , the effect of the coherent enhancement cannot be observed because its angular extent now spreads over the whole acceptance angle of the collecting optics. In the other limit, at large  $d$ , the transverse scattering length becomes larger than the size of the incident beam, and, accordingly, the coherent enhancement is limited to the angular width of a typical speckle.<sup>2</sup>

The case of interest in the present Letter is depicted in Fig. 1c. Continuing the line of qualitative reasoning, one can see that the overall effect of placing a RPS in front of the VSM is an increase in the separation distance  $\langle |\mathbf{r}_i - \mathbf{r}_f| \rangle$ . The phase difference between time-reversed paths is now the sum of contributions accumulated in the VSM and in the RPS. Evidently, when one or another contribution is stronger we recover the previous situations. For a weak RPS,  $\delta \ll l^*$ , the path-length distribution in the VSM remains practically unchanged and the enhancement peak is of the

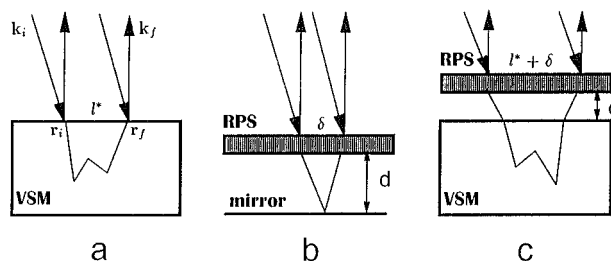


Fig. 1. Enhanced backscattering produced by coherent sources resulting from time-reversed pairs of light paths. Geometry of retroreflection from a, a VSM; b, a RPS placed close to a mirror; and c, a VSM placed behind a RPS.

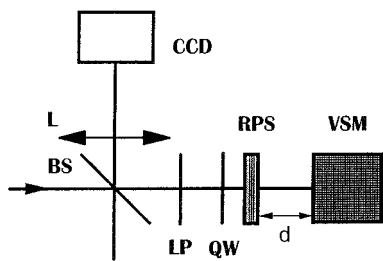


Fig. 2. Schematic of the experiment: BS, beam splitter; LP, linear polarizer; QW, quarter-wave plate; L, collecting lens.

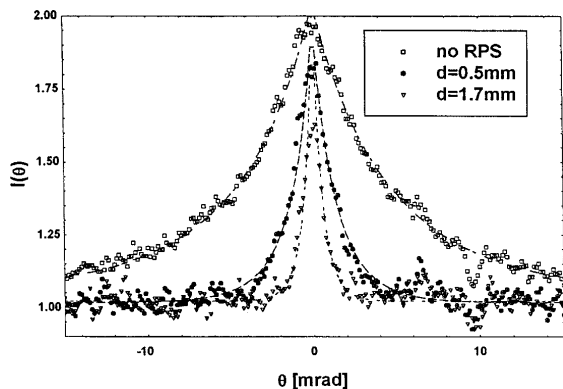


Fig. 3. Normalized cones of enhanced-backscattered intensity  $I(\theta)$  corresponding to scattering from a VSM alone and from different combinations of a VSM and a RPS as indicated. The experimental data (open symbols) are fitted to the theoretical model of Ref. 7 (dashed curves).

order of  $\lambda/l^*$ , as in Fig. 1a. When  $\delta \gg l^*$ , the path-length distribution is biased by the value of  $\delta$ , and the cone will be of the order of  $\delta/l^*$ . However, for intermediate cases, we can consider the enhancement peak as being produced by pairs of coherent sources with random azimuthal orientations and separated, on average, by a distance  $l_{app} = l^* + \delta$ . The overall effect is a narrowing of the coherence cone, which has now an angular extension of the order of  $\lambda/(l^* + 2\delta)$ .

We conducted a systematic experiment to study the effect of a combination of a RPS and a VSM on the shape and size of the peak of the enhanced-backscattered intensity. A schematic of the experimental setup is shown in Fig. 2. A collimated laser beam with  $\lambda = 633$  nm passes through a beam splitter and a circular polarization filter, which ensures that no single-scattering contributions are collected.<sup>4</sup> The circularly polarized beam further impinges upon a ground glass placed in front of the VSM. The retro-reflected light from the VSM passes again through the phase screen, is reflected by the beam splitter, and is then focused by a lens with 250-mm focal length onto the plane of a CCD array with  $520 \times 480$  pixels. In the experimental setup, no signal generated by scattering from RPS alone is observed. We performed an ensemble average by recording 40 different data frames while either rotating the VSM or translating the RPS across the optical axis. No significant differences were observed between these two modes of averaging.

In Fig. 3 we present typical cones of enhanced-backscattered intensity  $I(\theta)$  corresponding to different separation distances  $d$  as well as the cone corresponding to the case when no RPS was present in the optical path. Also shown are the fits of the recorded cones with a diffusion-theory model.<sup>7</sup> The narrowing of the enhancement cone when  $d$  increases is evident. An important observation is that, while the cone is shrinking, the functional form of the cone does not change; we fitted all the cones with the same theoretical expression. As opposed to absorption, finite-size,<sup>4</sup> and internal-reflection<sup>5</sup> effects, the magnitude of the enhancement peak is preserved in the limit of our experimental resolution. The EBS cone is essentially the Fourier transform of the distribution function of the separation distance between the end points of the time-reversed paths. Accordingly, the fact that all the cones in Fig. 3 have the same functional form implies that the photon-path distribution is not modified by the presence of a RPS. The RPS just adds a supplementary phase shift for all the photon paths. Placing a RPS leads to an increase of the apparent transport mean free path  $l_{app}$ . Increasing  $d$  reduces the width of the cone drastically. Eventually, the cone disappears at the angular extension of a typical speckle as expected.

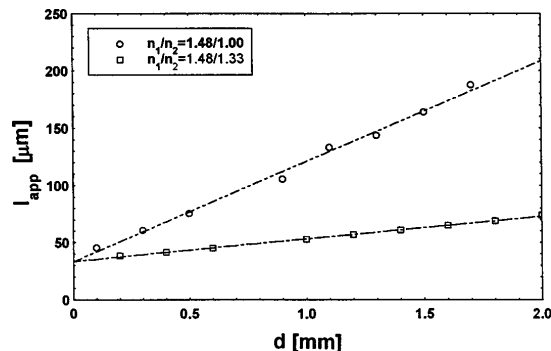


Fig. 4. Values of the apparent transport mean free path as a function of the separation distance between a VSM and a RPS. The circles correspond to a RPS determined by a glass-air interface, and the squares correspond to a RPS determined by a glass-water interface.

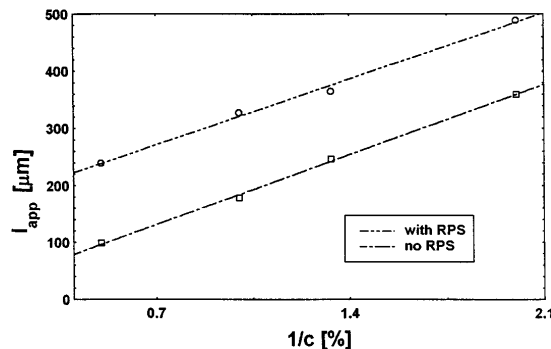


Fig. 5. Values of the apparent transport mean free path as a function of  $1/c$ , the inverse concentration of microspheres. The circles correspond to the combination of a VSM plus a RPS kept at a fixed distance  $d$ , and the squares correspond to the scattering from the VSM alone.

The dependence of  $l_{\text{app}}$  on separation  $d$  is presented in Fig. 4 for a RPS consisting of a ground-glass–air interface as well as a glass–water interface. The strength of the RPS can be easily adjusted by addition of thin films of liquids with known refractive indices.<sup>8</sup> The effect of the RPS phase-shift magnitude is evident: the stronger the phase distortion, the larger  $l_{\text{app}}$  corresponding to a narrower enhancement cone. A confirmation of the simple physical model in Fig. 1c is given by the linear dependence found experimentally between  $l_{\text{app}}$  and the separation distance  $d$ . Moreover, the slopes of the linear curves in Fig. 4 agree with our previous estimate  $l_{\text{app}}(d) \propto l^* + 2\epsilon(n_1/n_2 - 1)d$ . The ratio of the two slopes is 4.43, whereas an evaluation of  $(n_{\text{glass}}/n_{\text{air}} - 1)/(n_{\text{glass}}/n_{\text{water}} - 1)$  gives 4.25. Another important feature of the curves represented in Fig. 3 is the value of  $l_{\text{app}}$  extrapolated at  $d = 0$ . Both curves show  $l_{\text{app}}(d = 0) \approx 33 \mu\text{m}$ , which should be compared with the value of  $l^* = 27 \mu\text{m}$  obtained in the absence of the RPS. The small difference can be accounted for by reflection effects similar to those discussed in Ref. 6.

By examining the scattering geometry of Fig. 1c, one observes that even single-scattering events in a VSM may contribute to the final coherent enhancement seen from the double passage through the RPS. Contrary to EBS from a VSM alone, the single-scattering events in the VSM do not reduce the magnitude of the enhancement peak. However, the contribution of these scattering sequences is not dominant. To prove that, we conducted a different experiment designed to find whether one can still infer  $l^*$  corresponding to a VSM placed behind RPS with known properties. A glass cell with 1-cm thickness was filled with solutions of polystyrene microspheres and was placed behind a rotating ground-glass plate. During the experiment the distance between the RPS and the VSM (and therefore the shift  $\delta$ ) was kept constant. Solutions of polystyrene microspheres  $0.46 \mu\text{m}$  in diameter<sup>9</sup> and having concentrations  $c$  between 0.5 and 2% were used as a VSM. Values of  $l_{\text{app}}$  as inferred from the fit of the enhancement cones are presented in Fig. 5. The angular distribution of the scattered intensity was fitted with the same model,<sup>7</sup> but this time the fitting function was convolved with the finite experimental resolution of our apparatus. Also shown in Fig. 5 are the values of  $l_{\text{app}} = l^*$  corresponding to the case without a RPS present. As can be seen, in both cases we obtained a linear dependence between  $l_{\text{app}}$  and the inverse of the concentration, as expected for this low concentration of scatterers. The vertical shift between the two curves corresponds to the phase shift  $2\epsilon(n_1/n_2 - 1)d$  introduced by the phase screen. The results in Fig. 5 prove that, when a VSM is combined with a RPS, the total phase shift is a sum of the two contributions.

We suggest this approach to solve several problems that one encounters in using EBS to characterize the

scattering properties of random media. In spite of the great progress in understanding the physics of pure EBS, the direct application in materials characterization is hindered by several effects, such as sample geometry and reflection at the interface. In addition, most of the media of interest are solids with high density, and this presents experimental difficulties. The main problem is the need for an ensemble average, which one usually performs by simply moving the sample while recording several speckle patterns. In the experiment discussed in this Letter one can easily realize the average by rotating the RPS while keeping the VSM fixed.

A second characteristic of using the EBS technique on solid media is that usually the angular width is quite large, which imposes severe limitations on the optical apparatus used to record the angular variations of the scattered intensity. The ensemble VSM pulse RPS offers the possibility of being able to adjust the angular width of the peak to fall in the optimum range of the measuring apparatus.

When light propagates twice through a phase screen in its way to and from a multiple-scattering medium, the angular distribution of the retroreflected intensities is modified. The data summarized in Fig. 4 show that the width of the enhancement cone depends monotonically on the distance between a RPS and a VSM. Moreover, a simple model can be used to describe the influence of the phase-screen characteristics on this dependence. The cone-adjustment capabilities and the particular mode of ensemble averaging of this scheme can be successfully used for EBS evaluation on solid samples such as biological tissues,<sup>10</sup> aggregated media,<sup>11</sup> and random composites.<sup>12</sup>

## References

1. W. Goodman, *Statistical Optics* (Wiley, New York, 1985).
2. P. R. Tapster, A. R. Weeks, and E. Jakeman, *J. Opt. Soc. Am. A* **6**, 517 (1989).
3. B. S. Agrovskii, A. N. Boguratov, A. S. Gurrvich, S. V. Kireev, and V. A. Myakinin, *J. Opt. Soc. Am. A* **8**, 1142 (1991).
4. S. Etemad, R. Thompson, M. J. Andrejco, S. John, and F. C. MacKintosh, *Phys. Rev. Lett.* **59**, 1420 (1987).
5. P. M. Saulnier and G. H. Watson, *Opt. Lett.* **17**, 946 (1992).
6. M. Ospeck and S. Fraden, *Phys. Rev. E* **49**, 4578 (1994).
7. J. Z. Zhu, D. J. Pine, and D. A. Weitz, *Phys. Rev. A* **44**, 3948 (1991).
8. A. Dogariu, J. Uozumi, and T. Asakura, *Optik* **93**, 52 (1993).
9. Duke Scientific catalog number 3450A.
10. K. M. Yoo, G. C. Tang, and R. R. Alfano, *Appl. Opt.* **29**, 3236 (1990).
11. A. Dogariu, J. Uozumi, and T. Asakura, *Waves Random Media* **2**, 259 (1992).
12. A. Dogariu, J. Uozumi, and T. Asakura, *Part. Part. Syst. Charact.* **2**, 222 (1994).